Optimizing Solar Pond Design for Improved Thermal Storage Performance

[1]Dhiraj Kumar, [2]Dr Rashmi Dwivedi

[1]Department of Mechanical Engineering, Sri Satya Sai University of Technology and Medical Sciences Sehore (M.P.) India,
[2]Department of Mechanical Engineering, Sri Satya Sai University of Technology and Medical Sciences Sehore (M.P.) India,

Email [1]dhirajpoddar88@gmail.com, [2] rashmidwivedi29@gmail.com

* Corresponding Author: Dhiraj Kumar

Abstract: *This research investigates the thermal performance of various solar pond designs situated in central India (23° 18' 25" N, Longitude: 77° 23' 09'' E) through mathematical and computational fluid dynamics (CFD) analyses. Three-dimensional CFD models are developed for solar ponds without tubes, with serpentine tubes, and with spiral tubes, employing different heat transfer fluids, including water with varying salinity concentrations (NaCl 5% for NCZ & NaCl 10% for LCZ) and water with Al2O3 nano-fluid. The study reveals that the solar pond featuring a spiral tube and Al2O3 nano-fluid achieves the highest temperature generation and thermal efficiency compared to other designs. Future research avenues include exploring additional solar pond designs, investigating alternative nanofluids for enhanced heat transfer efficiency, and conducting experimental validation to refine computational models for practical applications.*

Keywords: *Solar ponds, Thermal performance, Mathematical analysis, Computational fluid dynamics (CFD).*

I. INTRODUCTION

The rise in global population has heightened the demand for energy, particularly in developed nations. This has spurred interest in renewable energy sources due to their environmental benefits and cost-effectiveness. Technologies like solar, wind, tidal, biomass, and geothermal energy are gaining traction for their sustainability. The past two decades have seen a surge in clean energy adoption, aligning with sustainable development goals and climate change mitigation efforts. Embracing renewable energy presents opportunities for social and economic development, improved energy security, and enhanced environmental and public health [1]. According to a projection by the World Energy Council [2], global electricity demand is expected to peak in 2030. India, a leading consumer of coal globally, heavily relies on costly imports of fossil fuels. Currently, about 74% of the nation's energy needs are met by coal and oil. A report from the Center for Monitoring Indian Economy reveals a significant increase in coal imports: 171 million tons in 2013–2014, 215 million tons in 2014–2015, 207 million tons in 2015–2016, 195 million tons in 2016–2017, and 213 million tons in 2017–2018 [3]. Solar power's widespread availability stands as a significant asset, despite the variations in solar radiation intensity caused by factors such as geographic location, time of day, and weather conditions. Areas near the equator consistently experience high levels of solar irradiance year-round, making them ideal for maximizing solar energy utilization [4].

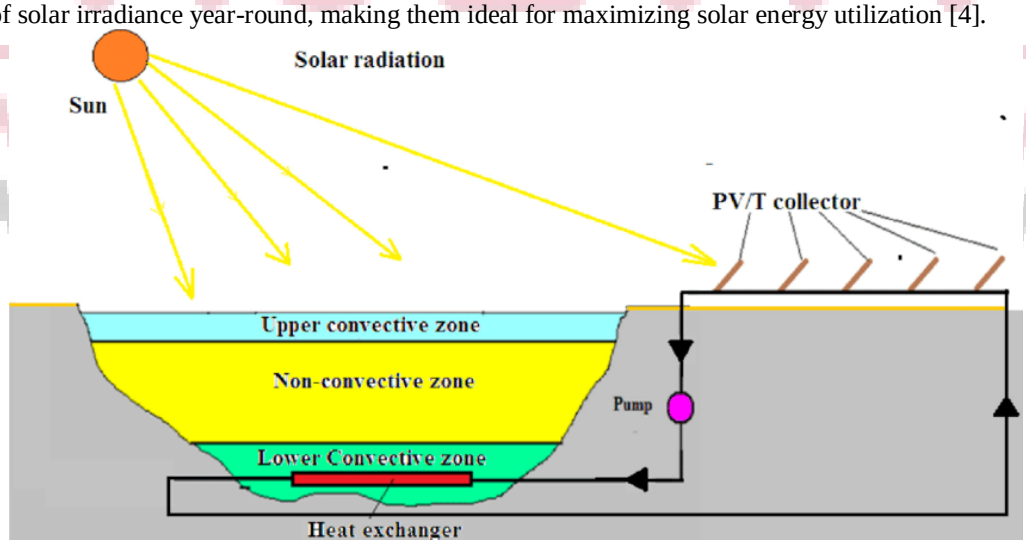

Fig. 1 Concept of Photovoltaic/Solar Pond (PVT/SP) [5]

A Solar Pond

Efficient capture and storage of thermal energy from solar radiation are essential considerations. One prominent device in this regard is the solar pond, recognized for its ability to gather thermal energy from sunlight. Typically characterized by substantial dimensions resembling a large pond, the solar pond utilizes a large saline reservoir to absorb and retain thermal energy in its warmer bottom storage zone. While solar ponds can occur naturally or be artificially constructed, contemporary applications predominantly favor artificial variants. A critical feature enabling their function as thermal energy storage systems is the presence of a salinity gradient, with highly concentrated saltwater in the lower convective zone (LCZ) and fresh water in the upper convective zone (UCZ). This salinity gradient facilitates convective heat transfer

between the zones, whereas in the non-convective zone (NCZ), heat transfer primarily occurs through conduction due to hindered convective currents [6].

This paper aims to enhance thermal storage performance by modifying solar pond design and integrating various heat transfer fluids. To achieve this goal, the research objectives encompass a multi-faceted approach. Firstly, mathematical analyses will be conducted at selected locations to evaluate key parameters such as radiations, reflection, refraction, and transmissivity. Subsequently, 3D CAD models will be developed to facilitate computational fluid dynamics (CFD) analysis of the solar pond, enabling a detailed examination of its thermal behavior. The CFD analysis will further explore maximum temperature variations under different water salinity concentrations and the incorporation of Al2O3 nano-fluid. Through this computational investigation, the study aims to gain insights into the effectiveness of various design modifications in enhancing thermal storage capabilities. Finally, the validity of the CFD results will be verified, and key performance metrics such as useful heat extraction rates and overall thermal efficiency of the solar pond will be determined, providing a comprehensive assessment of the proposed modifications.

II. LITERATURE REVIEW

Rghif, Y., et al. (2023) [7] investigated the influence of double-diffusive convection on the accuracy and computational efficiency of Salt Gradient Solar Pond (SGSP) simulations. They developed two numerical models using Fortran: a simple energy balance model neglecting double-diffusive convection, and a more complex model integrating Navier-Stokes, heat, and mass transfer equations to include double-diffusive convection effects. These models accounted for heat loss and internal heating dynamics. Experimental validation was performed using a scaled SGSP model over an 82-hour indoor test, demonstrating the effectiveness of both models in simulating SGSP thermal dynamics. The simpler model exhibited an average error of 9.39% in the Upper Convective Zone (UCZ) and 2.92% in the Lower Convective Zone (LCZ), while incorporating double-diffusive convection reduced errors to 5.98% for UCZ and 3.74% for LCZ. Notably, omitting double-diffusive effects led to a 4.3% overestimation in thermal energy storage. However, the more complex model required significantly greater computational resources, with processing times hundreds of times longer than the simpler approach. The integration of energy storage is pivotal in advancing solar energy technology, particularly to address its intermittent nature. Phase change materials (PCMs) have emerged as promising options for various solar energy systems. **Rashid, F.L.; et al. (2023) [8]** explored the extensive applications of PCMs across solar collectors, solar stills, solar ponds, solar air heaters, and solar chimneys. Despite challenges related to availability and cost, PCMs are widely used in solar energy techniques, contributing significantly to technical enhancements. While previous studies have focused on PCMs in photovoltaic systems, understanding their integration across diverse solar thermal energy systems is essential. Current research aims to enhance solar applications by investigating PCM use for thermal energy storage. Their study reviewed over 74 examples from open literature, demonstrating PCM maturity and successful integration into diverse solar energy applications, while suggesting future research directions. Residential water heating constitutes a substantial portion of total energy consumption in Australian buildings, prompting research into latent heat thermal energy storage (LHTES) systems to reduce fossil fuel reliance and promote renewable energy in solar water heating. However, current research primarily focuses on geometric optimization of LHTES heat exchangers, potentially overlooking comprehensive approaches for commercial implementation. **Modi, N., et al. (2023) [9]** provides insights into diverse solar hot water systems incorporating LHTES, emphasizing on-demand performance evaluations and structural optimizations to expedite commercial viability. The discussion in this perspective paper highlights challenges and references offering a comprehensive overview of LHTES-assisted solar hot water system performance, aiming to guide researchers towards developing energy-efficient solar hot water systems utilizing LHTES. **Ghazouani, N., et al. (2022) [10]**, emphasize the urgent need for swift water desalination solutions in the face of growing scarcity of potable water resources. They highlight the potential of humidification–dehumidification (HD) as a highly viable desalination method, particularly suitable for remote locations with modest freshwater requirements. Various solar-powered high-efficiency distillation (HD) desalination systems are explored, confirming the practicality of seawater HD systems in generating freshwater. Packed bed humidifiers and direct dehumidifiers are found to be effective components, with hybrid energy systems demonstrating superior gain output ratios (GOR). While HD shows promise for decentralized small-scale freshwater production, further improvements are needed for optimization both economically and in terms of gain output ratio. Salt Gradient Solar Pond (SGSP) systems offer a cost-effective means of capturing and storing solar energy. **Güven, P. (2018) [11]** investigates the experimental and numerical analysis of SGSPs, highlighting the coupled effects of solar radiation, wind speed, and ambient temperature on pond temperature. The study suggests exploring more detailed transient models and transparent cover materials to enhance stored sustainable energy and improve overall SGSP efficiency. In addressing challenges faced by solar energy conversion systems, **K.S. Reddy, et al. (2017) [12]**, examine the use of nanofluids and nanocomposites to enhance thermal and optical performance. Their work underscores the importance of these materials in increasing efficiency and reliability across low, medium, and high-temperature ranges in solar collectors. Nanofluids for heat transfer and nanocomposites as selective coatings emerge as promising approaches to elevate overall conversion efficiencies in solar energy systems.

III. METHODOLOGY

A solar pond is a reservoir of saline water designed to accumulate and retain solar thermal energy. The saltwater creates a vertical salinity gradient, with lower-salinity water positioned above higher-salinity water. The layers of salt solutions

progressively intensify in concentration and density as they extend deeper. Beyond a specific depth, the solution maintains a consistently high salt concentration.

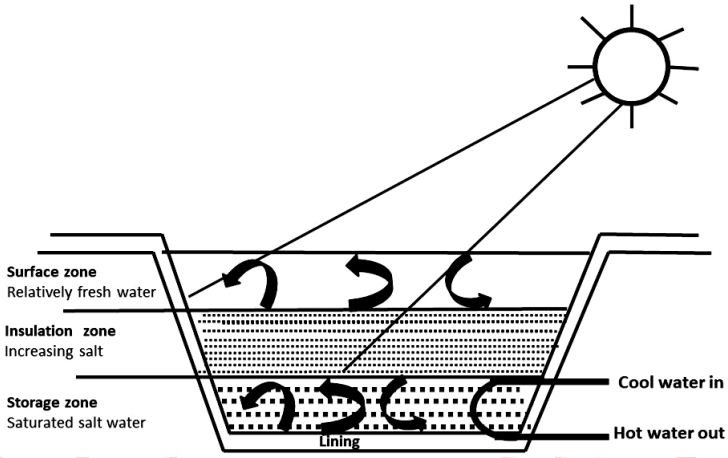

Fig. 2 Layer concept with salinity concentration of solar pond

CAD geometry of solar pond for design-1

A three-dimensional CAD model of a solar pond without a tube has been generated employing the ANSYS design module. The dimensional specifications for creating design-1 solar pond include a length and width of 1 m, a height of 0.5 m, and depths of 0.1 m, 0.3 m, and 0.1 m for the Upper Convective Zone (UCZ), Non-Convective Zone (NCZ), and Lower Convective Zone (LCZ), respectively, as illustrated in the figure.

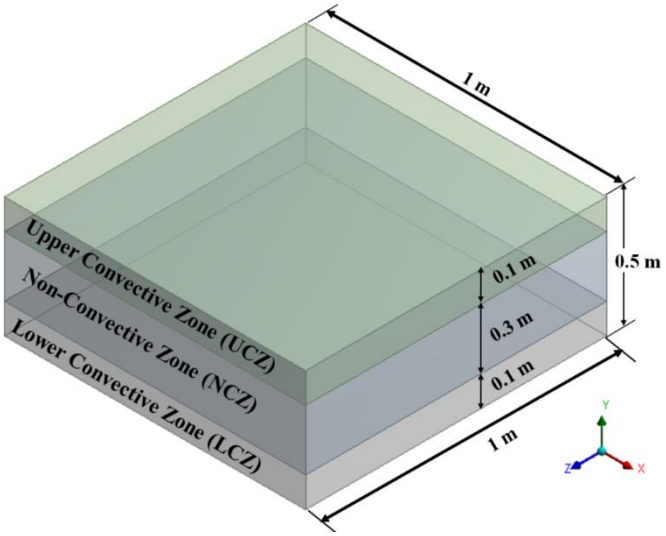

Fig. 3 CAD geometry of solar pond for design-1

The three-dimensional CAD model of the solar pond without a tube was generated using ANSYS Design Modular. Dimensional parameters for solar pond variant 1 included a length and width of 1 m each, a height of 0.5 m, and depths of 0.1 m, 0.3 m, and 0.1 m for the Upper Convective Zone (UCZ), Non-Convective Zone (NCZ), and Lower Convective Zone (LCZ), respectively (as depicted in the figure). Subsequently, the CAD geometry underwent meshing, dividing the geometry into nodes and elements. The resulting mesh comprised 202,848 nodes and 44,180 hexahedral elements.

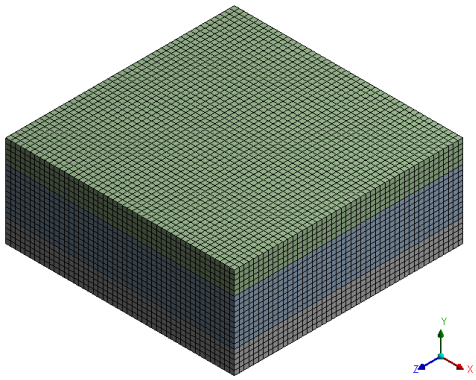

Fig. 4 Meshing of solar pond for design-1

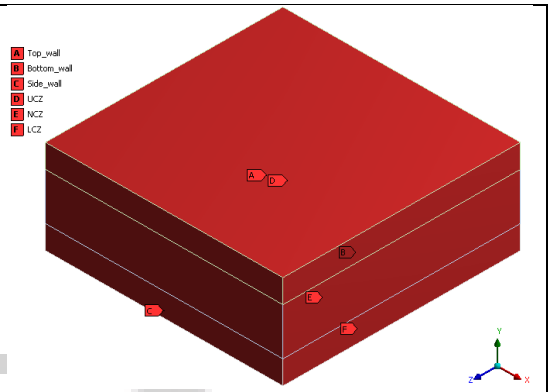

Fig. 5 Different domain and boundaries of solar pond for design-1

CAD geometry for solar pond design-2

A three-dimensional CAD model of a solar pond with a serpentine tube was created using ANSYS Design Modular. Specifications for design variant 2 included a length and width of 1 meter each, with a height of 0.5 meters. Depths of the Upper Convective Zone (UCZ), Non-Convective Zone (NCZ), and Lower Convective Zone (LCZ) were 0.1 meters, 0.3 meters, and 0.1 meters, respectively. The serpentine tube had a diameter of 25 millimeters and comprised 12 turns, as illustrated in the technical diagram.

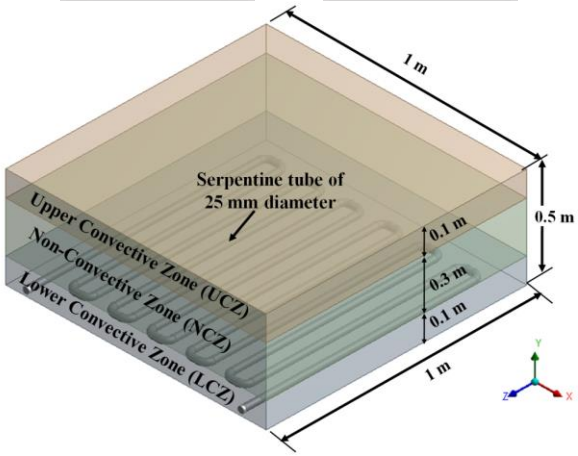

Fig. 6 CAD geometry of solar pond for design-2

After developing the three-dimensional CAD model of the solar pond with a serpentine tube for design-2, the geometry underwent meshing. Meshing is a critical process where the CAD geometry is divided into nodes and elements. In this study, the mesh consisted of 2,767,916 nodes and a total of 814,337 elements. Hexahedral and tetrahedral elements were employed to address the complexity of the Lower Convective Zone (LCZ).

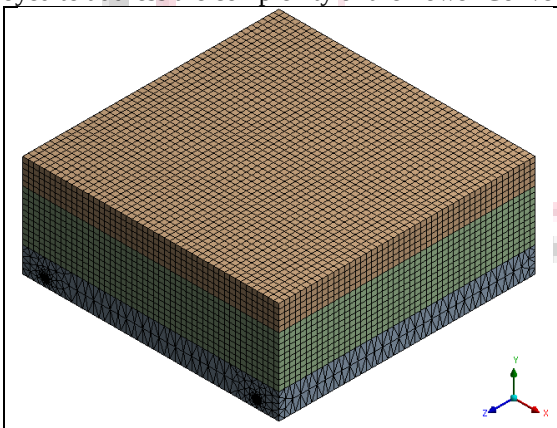

Fig. 7 Meshing of solar pond for design-2

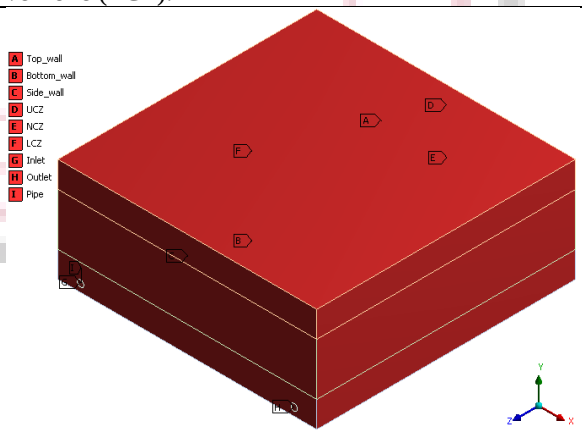

Fig. 8 Different domain and boundaries of solar pond for design-2

CAD geometry for solar pond design-3

A three-dimensional CAD model of a solar pond with a spiral tube was created using ANSYS Design Modular. Design-3 specifications for the solar pond included a length and width of 1 meter, a height of 0.5 meters, and depths of 0.1 meters,

0.3 meters, and 0.1 meters for the Upper Convective Zone (UCZ), Non-Convective Zone (NCZ), and Lower Convective Zone (LCZ), respectively. The spiral tube featured a diameter of 25 mm with 8 coils, as depicted in the figure.

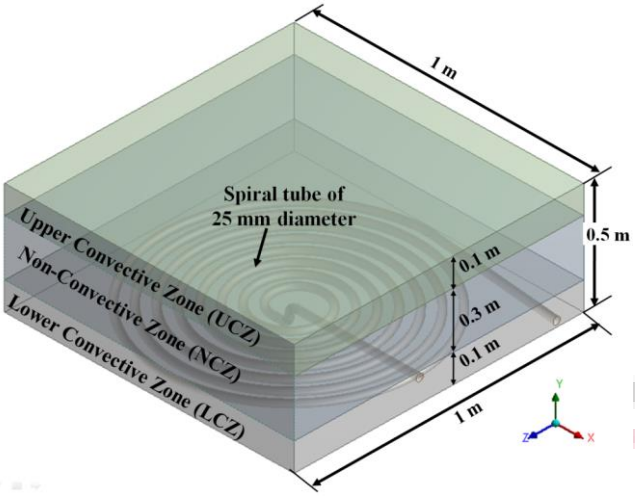

Fig. 9 CAD geometry of solar pond for design-3

After developing the three-dimensional CAD model for design-3 of the solar pond with a spiral tube, the model was meshed. Meshing divides the CAD geometry into nodes and elements. In this study, meshing produced 1,045,105 nodes and 559,134 elements. Hexahedral and tetrahedral elements were employed to handle the complexity of the Lower Convective Zone (LCZ).

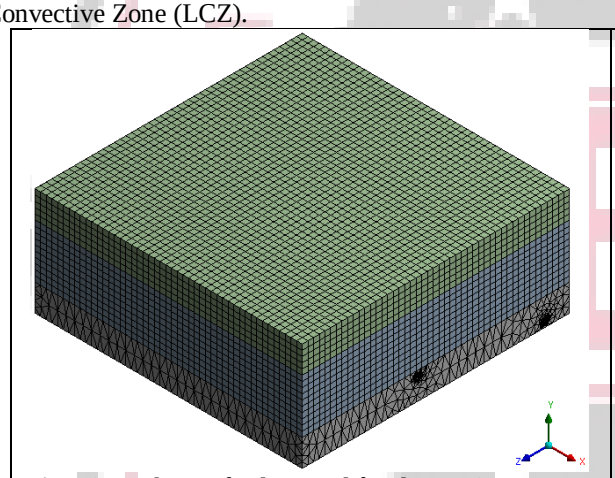

Fig. 10 Meshing of solar pond for design-3

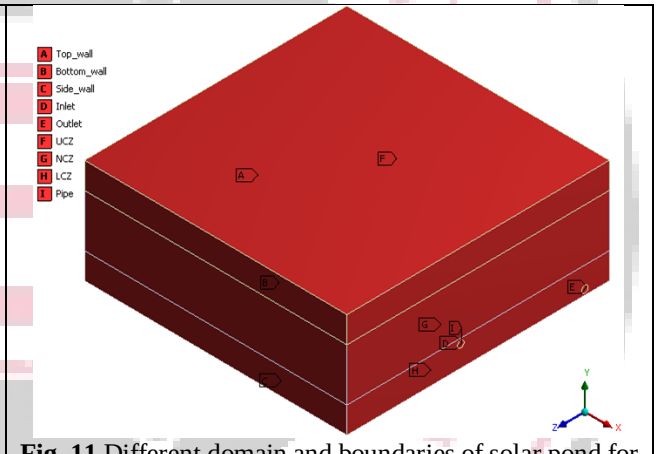

Fig. 11 Different domain and boundaries of solar pond for design-3

Analysis of contours and graphical diagrams reveals a 6.5% variation in the number of quadrilateral elements and a maximum temperature variation of 0.8% compared to the base paper. These results demonstrate strong agreement between the present study and published literature, warranting further analysis of different solar pond designs under the same boundary conditions.

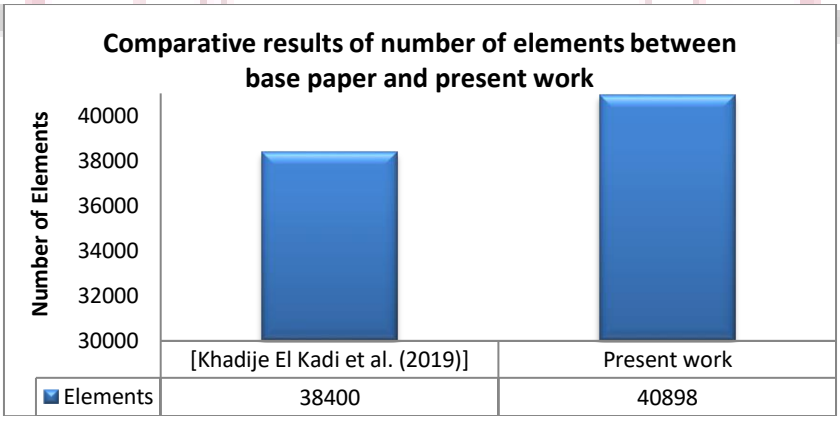

Fig. 12 Comparative results of number of elements between base paper and present work

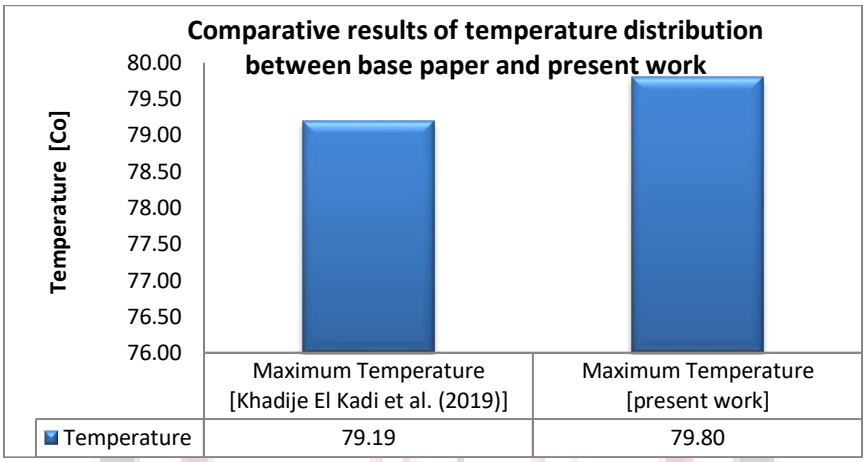

Fig. 13 Comparative results of temperature distribution between base paper and present work

IV. RESULT AND DISCUSSION

In this study, we aimed to enhance the thermal storage efficiency of solar ponds through comprehensive mathematical and computational fluid dynamics (CFD) analysis. Three distinct three-dimensional CFD models were developed: one without pipes, one with a serpentine tube, and one with a spiral tube. We compare the thermal performance of these designs and discuss their implications, shedding light on their storage capabilities.

Calculation of declination angle

$$Declination\ Angle\ (\delta) = 23.45\ \sin\left[\frac{360}{365}(284 + n)\right]$$

Note: First month = Jan, Twelfth Month = December

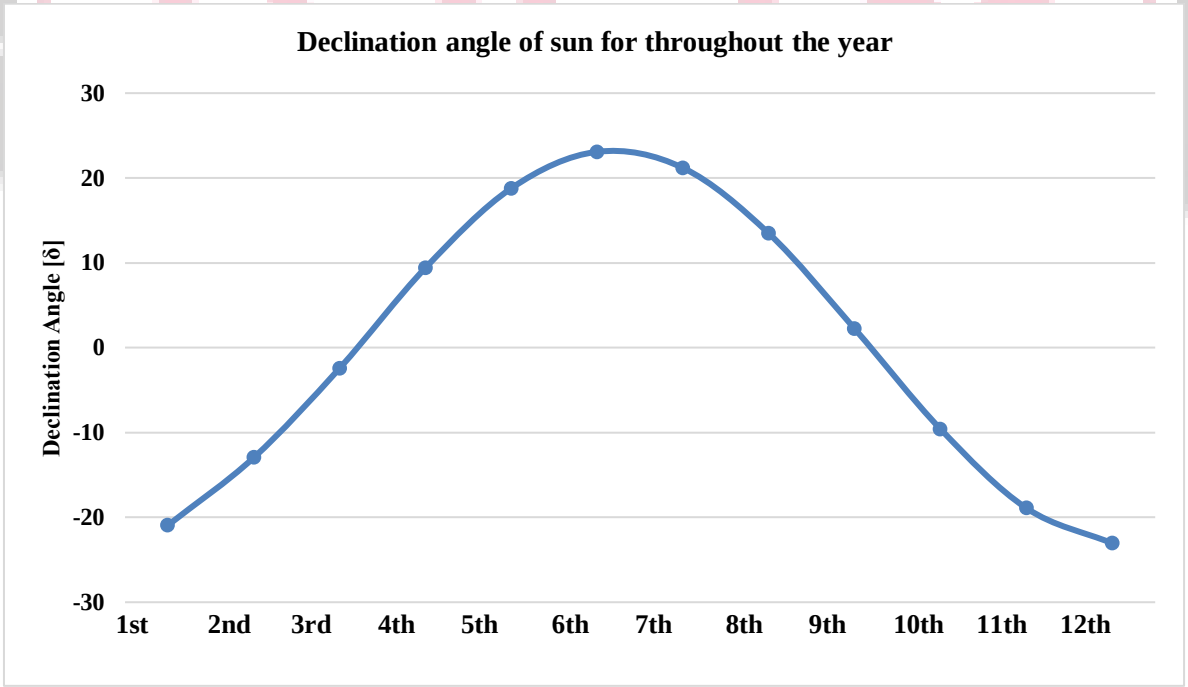

Fig. 14 Calculated Declination angle of sun for throughout the year

The graph shows monthly declination angles (δ), representing the vertical tilt of the sun's rays influenced by Earth's axial tilt. Angles start negative from January to March, peak positively in June, then decrease, turning negative again by October and December.

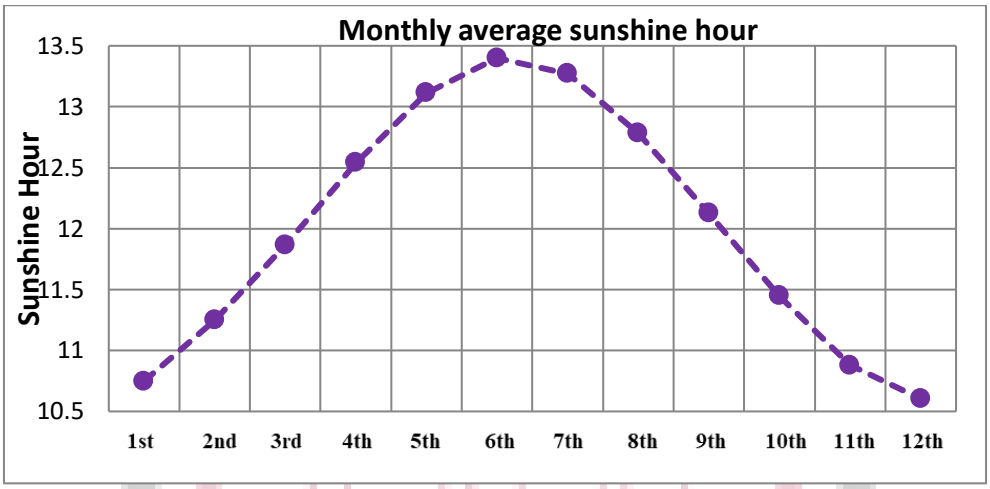

Fig. 15 Monthly average sunshine hour

Figure 15 shows monthly sunshine hours (Smax) throughout the year, indicating the duration of sunlight received at a specific location. The data highlights variations in sunlight exposure, with notable peaks in the third and seventh months and lower values in the eleventh and twelfth months. Understanding these variations is crucial for assessing seasonal changes and their implications for solar energy and climate considerations.

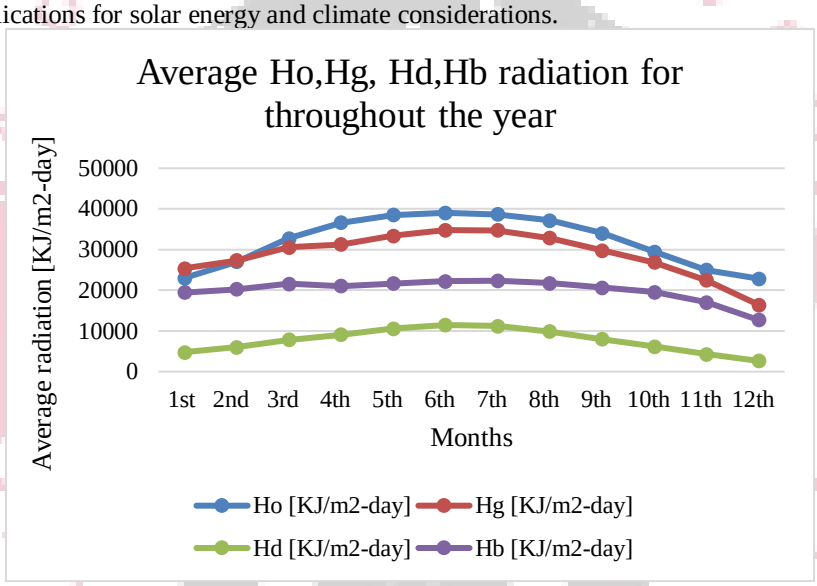

Fig. 16 Average Ho,Hg, Hd,Hb radiation for throughout the year

Computational fluid dynamic analysis of solar pond for design-1

After completing computational fluid dynamics (CFD) analysis for a tubeless solar pond configuration, a detailed examination of temperature distribution across the Lower Convective Zone (LCZ), Non-Convective Zone (NCZ), and Upper Convective Zone (UCZ) was conducted. Water with varying salinity concentrations (5% NaCl for NCZ and 10% NaCl for LCZ) was used in different layers. Results revealed distinct temperature profiles within the solar pond, with the LCZ reaching the highest recorded temperature of 79.91 degrees Celsius and the uppermost layer of the UCZ registering the lowest temperature at 40 degrees Celsius. These insights, depicted in Figures 5.21 and 5.22, elucidate the thermal behavior of the tubeless solar pond under different salinity conditions across its layers.

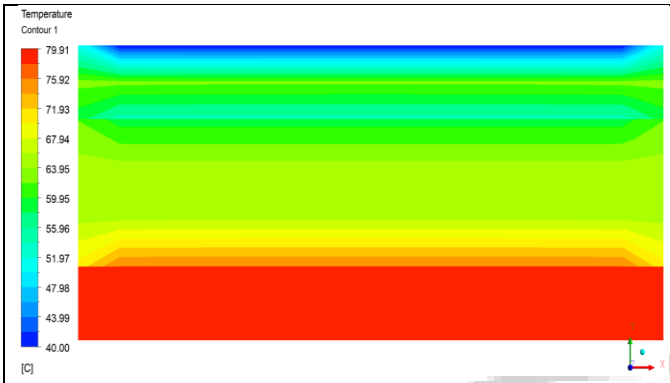

Fig. 17 Temperature distribution on different layer of solar pond using different salinity concentration for design-1

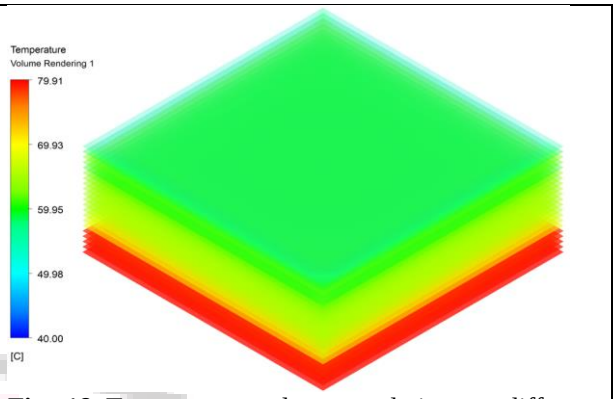

Fig. 18 Temperature volume rendering on different layer of solar pond using different salinity concentration for design-1

After completing computational fluid dynamics (CFD) analysis on a tubeless solar pond, the temperature distribution across layers—Lower Convective Zone (LCZ), Non-Convective Zone (NCZ), and Upper Convective Zone (UCZ)—was examined. This analysis involved using water infused with Al2O3 nano-fluid. Results revealed distinct thermal profiles, with the LCZ reaching a peak temperature of 82 degrees Celsius and the UCZ's uppermost layer registering a minimum temperature of 40 degrees Celsius. Visual representations of these variations are shown in Figures 5.23 and 5.24. The inclusion of Al2O3 nano-fluid significantly influenced the thermal characteristics of the solar pond, providing valuable insights into temperature dynamics in the absence of tubes.

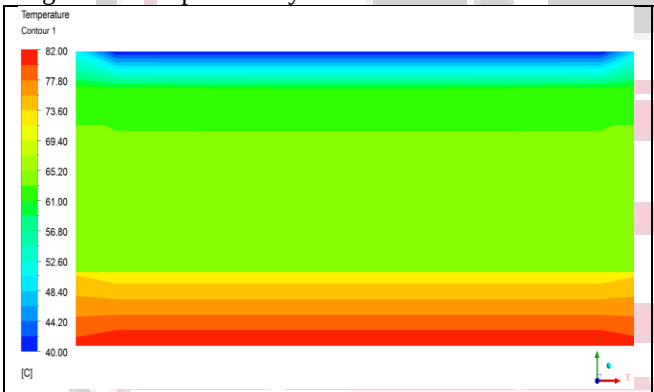

Fig. 19 Temperature distribution on different layer of solar pond using Al2O3 for design-1

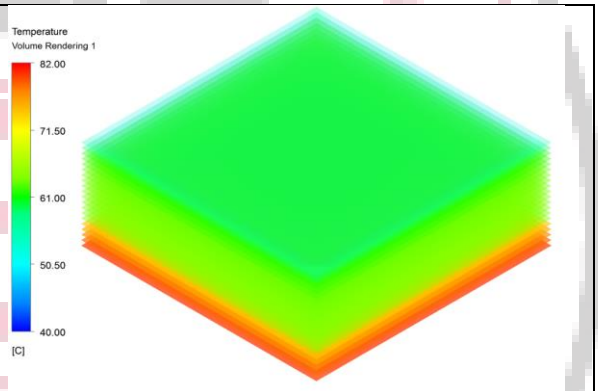

Fig. 20 Temperature volume rendering on different layer of solar pond using Al2O3 for design-1

CFD Analysis of Solar Pond Design-2

Following a computational fluid dynamics analysis of a solar pond with a serpentine tube, the temperature distribution across layers—Lower Convective Zone (LCZ), Non-Convective Zone (NCZ), and Upper Convective Zone (UCZ)—was examined. Different salinity concentrations (NaCl 5% for NCZ and NaCl 10% for LCZ) were applied to these layers. Results showed notable thermal profiles, with the LCZ reaching a peak temperature of 82.16 degrees Celsius, while the top layer of the UCZ recorded the lowest temperature at 40 degrees Celsius. Visual representations of these variations can be seen in Figures 21 and 22.

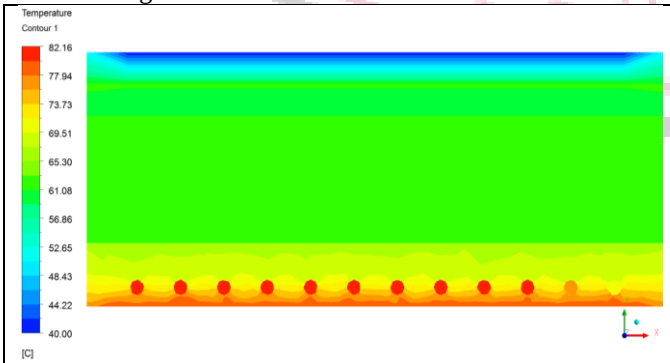

Fig. 21 Temperature distribution on different layer of solar pond using different salinity concentration for design-2

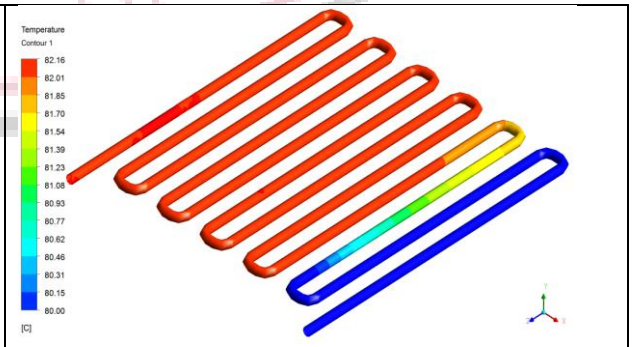

Fig. 22 Temperature volume rendering on different layer of solar pond using different salinity concentration for design-2

After conducting a computational fluid dynamics analysis on a solar pond with a serpentine tube, we examined the temperature distribution across different layers: the Lower Convective Zone (LCZ), Non-Convective Zone (NCZ), and Upper Convective Zone (UCZ). This analysis utilized water infused with Al2O3 nano-fluid. Results revealed distinct thermal profiles, with the LCZ recording the highest temperature at 84.61 degrees Celsius, while the uppermost layer of the UCZ exhibited the lowest temperature at 40 degrees Celsius. Visual representations of these variations can be found in Figures 23 and 24.

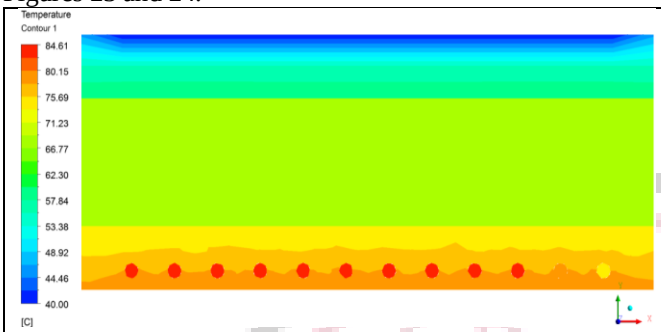

Fig. 23 Temperature distribution on different layer of solar pond using Al2O3 for design-2

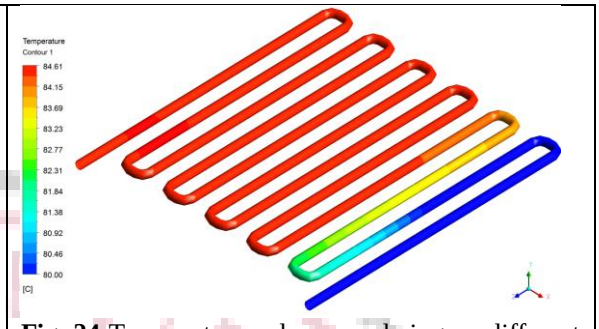

Fig. 24 Temperature volume rendering on different layer of solar pond using Al2O3 for design-2

Computational fluid dynamic analysis of solar pond for design-3

After completing computational fluid dynamics analysis on a solar pond with a spiral tube, we examined temperature distribution across layers: Lower Convective Zone (LCZ), Non-Convective Zone (NCZ), and Upper Convective Zone (UCZ). Varying salinity concentrations (NaCl 5% for NCZ and NaCl 10% for LCZ) were applied. Results revealed distinctive thermal profiles, with the mid-plane registering the highest temperature at 91.26 degrees Celsius, while the top layer exhibited the lowest temperature at 40 degrees Celsius. Visual representations of these variations can be found in Figures 25 and 26. The integration of a spiral tube and varying salinity concentrations influenced the solar pond's thermal behavior, providing valuable insights into temperature dynamics across its layers.

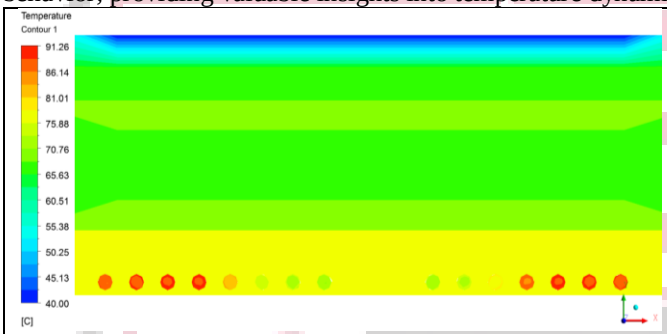

Fig. 25 Temperature distribution on different layer of solar pond using different salinity concentration for design-3

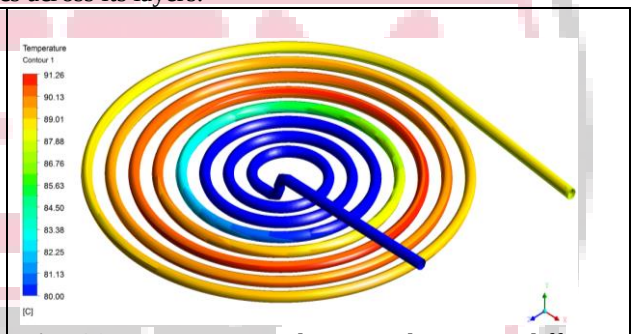

Fig. 26 Temperature volume rendering on different layer of solar pond using different salinity concentration for design-2

Following a computational fluid dynamics analysis on a solar pond with a spiral tube, temperature distribution across layers—Lower Convective Zone (LCZ), Non-Convective Zone (NCZ), and Upper Convective Zone (UCZ)—was examined. Water with Al2O3 nano-fluid was used. Results showed distinct thermal profiles, with the LCZ recording the highest temperature at 93.75 degrees Celsius, while the top layer of the UCZ exhibited the lowest temperature at 40 degrees Celsius. Visual representations of these variations can be seen in Figures 27 and 28. The integration of a spiral tube and Al2O3 nano-fluid significantly influenced the solar pond's thermal characteristics, providing valuable insights into temperature dynamics across its layers.

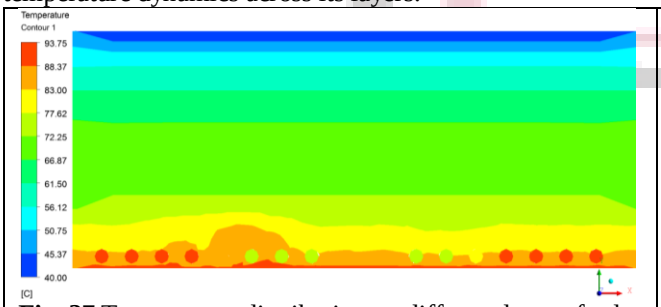

Fig. 27 Temperature distribution on different layer of solar pond using Al2O3 for design-3

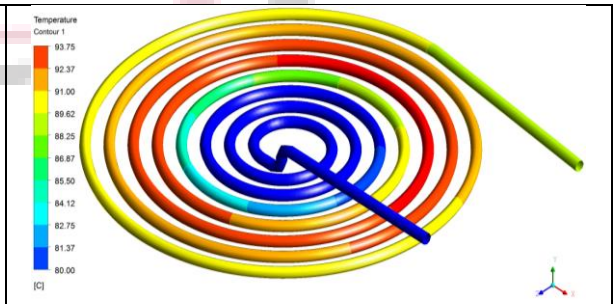

Fig. 28 Temperature volume rendering on different layer of solar pond using Al2O3 for design-3

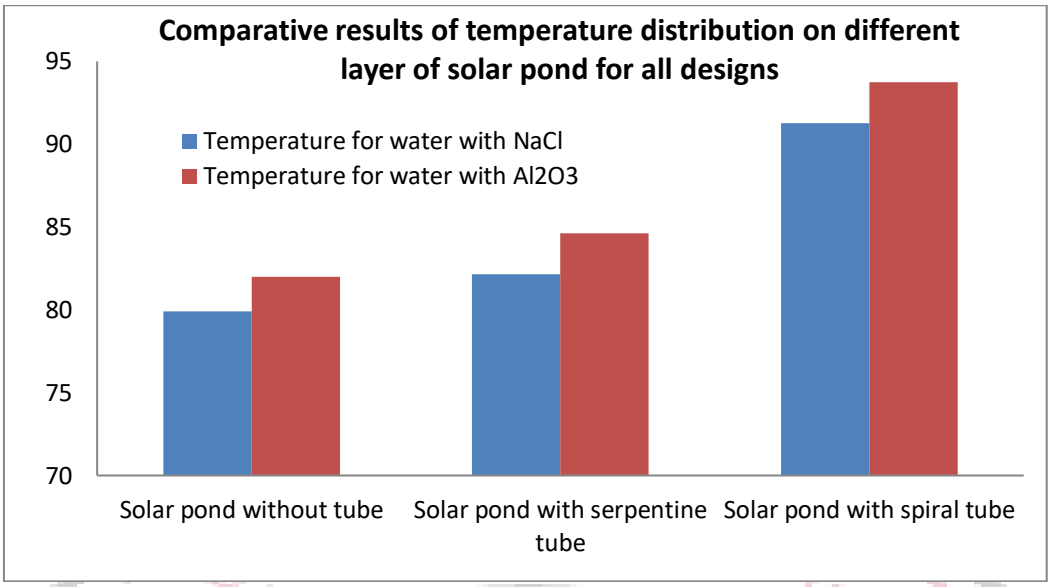

Fig. 29 Comparative results of temperature distribution on different layer of solar pond for all designs

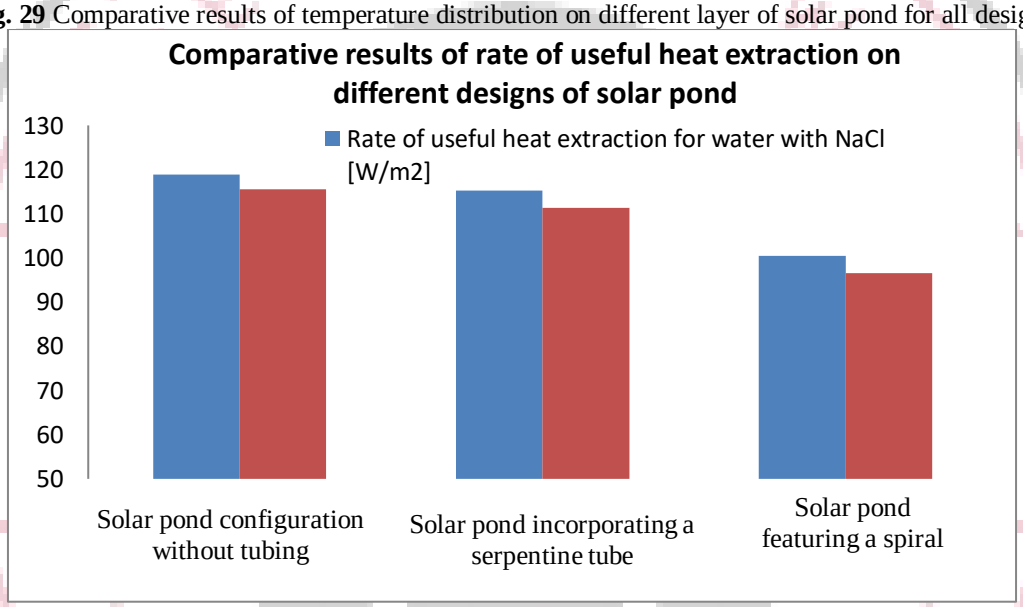

Fig. 30 Comparative results of rate of useful heat extraction on different designs of solar pond

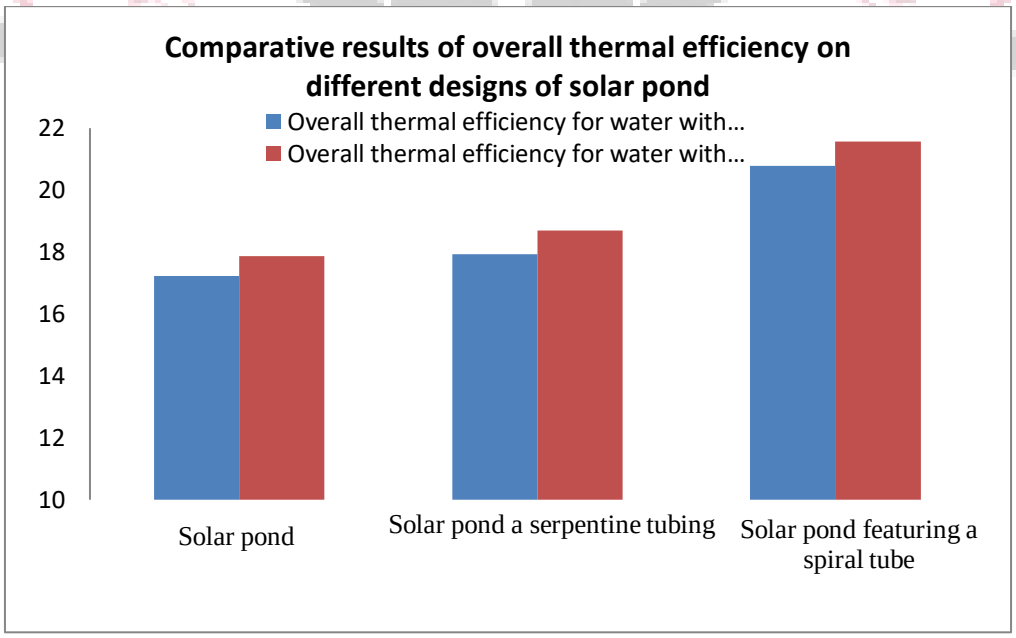

Fig. 31 Comparative results of overall thermal efficiency on different designs of solar pond

V. Conclusion

In this study, mathematical and computational fluid dynamics (CFD) analyses were conducted on various solar pond designs at the location of central India (23° 18' 25" N, Longitude: 77° 23' 09'' E). Three-dimensional CFD models were developed for solar ponds without tubes, with serpentine tubes, and with spiral tubes, using different heat transfer fluids, including water with varying salinity concentrations (NaCl 5% for NCZ & NaCl 10% for LCZ) and water with Al2O3 nano-fluid. Key findings revealed that the solar pond with a spiral tube and Al2O3 nano-fluid demonstrated the highest temperature generation and thermal efficiency among all designs. Future research avenues include exploring additional solar pond designs, investigating alternative nanofluids for enhanced heat transfer efficiency, and conducting experimental validation to refine computational models for practical applications.

References

[1] Subhashish Dey, Anduri Sreenivasulu, G.T.N. Veerendra, K. Venkateswara Rao, P.S.S. Anjaneya Babu, Renewable energy present status and future potentials in India: An overview, Innovation and Green Development, Volume 1, Issue 1, 2022, 100006, ISSN 2949-7531, https://doi.org/10.1016/j.igd.2022.100006.

[2] World Energy Scenarios Composing energy futures to 2050 (2013), World energy Council. https://www.worldenergy.org/wp-content/uploads/2013/09/World-Energy-Scenarios_Composing-energy-futures-to-2050_Full-report.pdf

[3] Blondeel, M., & Van de Graaf, T. (2018). Toward a global coal mining moratorium? A comparative analysis of coal mining policies in the USA, China, India and Australia. Climatic Change, 150(1-2), 89-101.

[4] Reames, T. G. (2020). Distributional disparities in residential rooftop solar potential and penetration in four cities in the United States. Energy Research & Social Science, 69, 101612.

[5] Ali, Manar & Ahmed, Omer & Fadhil, Ehsan. (2020). Performance of solar pond integrated with photovoltaic/thermal collectors. Energy Reports. 6. 10.1016/j.egyr.2020.11.037.

[6] Ranjan Das, Sayantan Ganguly, A comprehensive review on solar pond research in India: Past, present and future, Solar Energy, Volume 247, 2022, Pages 55-72, ISSN 0038-092X, https://doi.org/10.1016/j.solener.2022.10.008.

[7] Rghif, Y., Colarossi, D., & Principi, P. (2023). Effects of Double-Diffusive Convection on Calculation Time and Accuracy Results of a Salt Gradient Solar Pond: Numerical Investigation and Experimental Validation. Sustainability, 15(2), 1479.

[8] Rashid, F.L.; Al-Obaidi, M.A.; Dulaimi, A.; Bahlol, H.Y.; Hasan, A. Recent Advances, Development, and Impact of Using Phase Change Materials as Thermal Energy Storage in Different Solar Energy Systems: A Review. Designs 2023, 7, 66. https://doi.org/10.3390/ designs7030066

[9] Modi, N., Wang, X., & Negnevitsky, M. (2023). Solar Hot Water Systems Using Latent Heat Thermal Energy Storage: Perspectives and Challenges. Energies, 16(4), 1969.

[10] Ghazouani, N., El-Bary, A. A., Hassan, G. E., Becheikh, N., Bawadekji, A., & Elewa, M. M. (2022). Solar Desalination by Humidification–Dehumidification: A Review. Water, 14(21), 3424.

[11] Güven, P. (2018). Experimental and numerical analysis of a salt gradient solar pond (Master's thesis, Middle East Technical University.

[12] K.S. Reddy, Nikhilesh R. Kamnapure, Shreekant Srivastava, Nanofluid and nanocomposite applications in solar energy conversion systems for performance enhancement: a review, International Journal of Low-Carbon Technologies, Volume 12, Issue 1, March 2017, Pages 1–23, https://doi.org/10.1093/ijlct/ctw007

[13] Khadije El Kadi et al. (2019) "Flow simulation and assessment of a salinity gradient solar pond development" Energy Procedia 158 (2019) 911–917. Doi: 10.1016/j.egypro.2019.01.230.